HIP ARTHROPLASTY

Biomechanical analysis of different THA cementless femoral stem designs in physiological and osteoporotic bone during static loading conditions

Matteo Formica[1,2] · Andrea Zanirato[1,2] · Edoardo Bori[3] · Tullio Andrea Revetria[1,2] · Juljana Ditting[3] · Bernardo Innocenti[3]

Abstract

Background The influence of THA stem design on periprosthetic femoral fractures (PFFs) risk is subject of debate. This study aims to compare the effects of different cementless stem designs on stress–strain distributions in both physiological and osteoporotic femur under various loading conditions.

Materials A biomechanical study using finite-element analysis was conducted. Four models were developed: three with implanted femurs and a native one chosen as control. Each model was analyzed for both healthy and osteoporotic bone. The following stem designs were examined: short anatomical stem with femoral neck preservation, double-wedge stem, and anatomical standard stem. Three loading conditions were assessed: gait, sideways falling, and four-point bending.

Results During gait in physiological bone, the anatomical stem and the short anatomical stem with femoral neck preservation showed stress distribution similar to the native model. The double-wedge stem reduced stress in the proximal area but concentrated it in the meta-diaphysis. In osteoporotic bone, the double-wedge stem design increased average stress by up to 10%. During sideways falling, the double-wedge stem exhibited higher stresses in osteoporotic bone. No significant differences in average stress were found in any of the studied models during four-point bending.

Conclusion In physiological bone, anatomical stems demonstrated stress distribution comparable to the native model. The double-wedge stem showed uneven stress distribution, which may contribute to long-term stress shielding. In the case of osteoporotic bone, the double-wedge stem design resulted in a significant increase in average stress during both gait and sideways falling, potentially indicating a higher theoretical risk of PFF.

Keywords THA · Periprosthetic femoral fractures · Cementless · Stem design

Introduction

Total hip arthroplasty (THA) is considered as one of the most successful surgical procedures of the last century. The increasing global need for this type of surgical procedure is clearly reflected in the arthroplasty registries [1–4].

The choice between cemented and cementless implant fixation strategies, along with the materials and design of prosthetic femoral components, is a subject of various discussions within the research community [5–10]. These discussions are focused on exploring the link between implant characteristics and their corresponding outcomes, encompassing performance and the possibility of potential failure. Among the different causes of implant failure, periprosthetic femoral fractures (PFF) represent one of the most common reasons leading to THA revision [1]. The

✉ Edoardo Bori
  edoardo.bori@gmail.com

1 Dipartimento di Scienze Chirurgiche e Diagnostiche Integrate (DISC), Università Degli Studi di Genova, Viale Benedetto XV N°6, 16132 Genoa, Italy

2 IRCCS Ospedale Policlinico San Martino, UO Clinica Ortopedica, Largo Rosanna Benzi N° 10, 16132 Genoa, Italy

3 BEAMS Department (Bio Electro and Mechanical Systems), École Polytechnique de Bruxelles, Université Libre de Bruxelles, Av. F. Roosevelt, 50 CP165/56, 1050 Brussels, Belgium

incidence of this complication seems to be on the rise, as indicated by data from arthroplasty registries showing a progressively increasing rate of 4.6% per decade for the upcoming 3 decades [11].

In contrast to cemented implants, cementless femoral components depend on the press-fit method for initial stability, which subsequently transitions into secondary stability through osteointegration [8]. However, these types of implants have been linked to a greater occurrence of periprosthetic femoral fractures during surgery and shortly after (within the initial 6 months, thus before full osteointegration occurs), when compared to cemented prostheses [12–15]. Nevertheless, the trend toward the use of cementless implants is still rising [5].

Nowadays, the market provides a variety of cementless stem designs characterized by varying lengths and shapes. However, the impact of these attributes on the risk of PFF remains a subject of ongoing discussion in the literature [13–15]. Consequently, the aim of this study is to compare the biomechanical effects induced by different cementless hip stems designs: this assessment will focus on the distribution of stress and strain, considering both physiological and osteoporotic bones, and will be conducted under a variety of loading conditions.

The main target of this study will be the first perioperative period, i.e., after the prosthesis implantation but prior to the occurrence of osteointegration. Addressing this timeframe, it's worth noting in the literature that PFFs observed within the immediate month following the operation might have originated during surgery itself as minor cracks or fissures, subsequently progressed into clinical fractures during the rehabilitation period [12, 14, 15]. Another possible reason leading to this kind of PFFs can then be related to errors in the choice of the proper implant size, as under-sizing was proven to be related to generation of new fracture rhymes [12, 14, 15].

Long-term post-operative PFF, on the other hand, might be a consequence of failed stem osteointegration, bone overload and consequently mechanical failure [14]. However, data from the Nordic Arthroplasty Register indicated that the vast majority of these fractures manifested within the initial six months following the surgical procedure [15]. Consequently, these studies confirm that the period before stem osteointegration stands as the main critical phase in uncemented THA and thus justifies the choice of this study to address it (therefore, not considering osteointegration itself or other long-term processes due to eventual implant coatings).

In order to achieve this goal, an in-silico biomechanical study based on finite-element analysis was performed: this approach, well established in the current literature, was chosen for the great comparative potential it provides. It allows indeed to change each single parameter of the model in order to precisely analyze its influence on the outcomes, while leaving the other boundary conditions unchanged [16, 17].

Materials and methods

The models were implemented as follows.

Geometry

For the bone geometry, a physiological three-dimensional femur model was reconstructed from CT-scans of a right femur mechanical-equivalent synthetic bone (Sawbones Europe AB, Limhamn, Sweden). The use of this kind of femoral models is widely adopted in the literature thanks to their excellent capability of standardizing results [18–24], and these reproductions are based on physiological geometries of cortical bone, cancellous bone and intramedullary canal; these geometries were then analyzed and returned a Dorr's ratio of 0.55 [25].

Three different THA stem designs from the same manufacturer (Waldemar Link GmbH & Co. KG, Hamburg, Germany) were implemented: a short anatomical stem with femoral neck preservation (C.F.P. II) (see Fig. 1A) and two standard cementless femoral stems: a double-wedge stem (LCU) (see Fig. 1B) and an anatomical standard stem (SP-CL) (see Fig. 1C), respectively, Type 2 and Type 6 accordingly to Khanuja and Mont [26]. The size of the hip stems was chosen in agreement with the size of the bone model.

Following the manufacturer surgical technique, each stem was virtually implanted in the femoral bone and the configuration obtained was validated by an expert hip surgeon (M.F.).
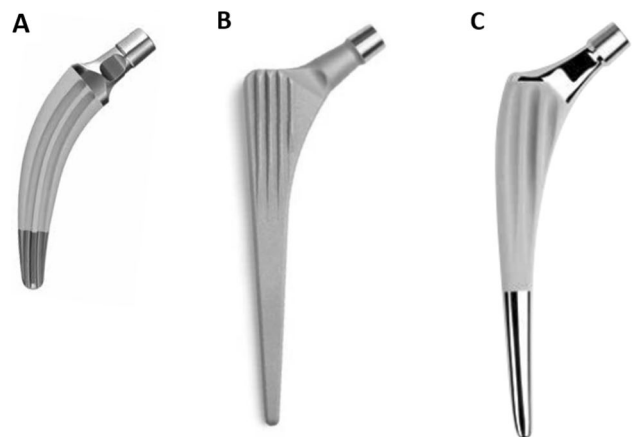

Fig. 1 The THA stem designs analyzed: a short anatomical stem with femoral neck preservation (**A**), a Type 2 stem (**B**) and a Type 6 stem (**C**)

Material models and properties

Linear elasticity was used for all the material models considered in this study.

For the physiological bone quality, the cortical bone was considered transversely isotropic and the following material properties were used: $E1 = E2 = 11.5$ GPa, $E3 = 17$ GPa, $\nu12 = 0.51$, $\nu23 = \nu13 = 0.31$ [26]; the third axis was considered as parallel to the anatomical axis of the femur. The cancellous bone was instead considered isotropic with $E = 2.13$ GPa, $\nu = 0.3$ [19, 27].

To simulate osteoporotic material properties, according to literature [19], the Young's modulus of cortical bone was reduced by 32% whereas the Young's modulus of cancellous bone was reduced by 66%. Consequently, the Young's modulus for osteoporotic cortical bone is $E1 = E2 = 7.82$ GPa, $E3 = 11.56$ GPa while for osteoporotic cancellous bone it is $E = 724$ MPa. The Poisson's ratio remains the same for both healthy and osteoporotic bone qualities [18, 19].

The material for all the stems implemented was Titanium alloy, considered as isotropic with $E = 105$ GPa, $\nu = 0.34$ [28].

A coefficient of friction of 0.2 was considered among the stem and the bone, in order to simulate the cementless implantation technique [27].

Boundary conditions

Each model was then tested under the following load conditions:

1. *Gait cycle* this test evaluates the outcomes during the most common daily activity, by analyzing the effects of the maximum force involved in such task. A body weight of 800 N is considered as a reference to define the loads applied to the femoral head, to the great trochanter and to the vastus lateralis, in according to what was reported in the literature [19, 29]. The distal part of the femur is fully constrained, and the three forces are applied on the relative landmarks of the proximal side (Table 1): the femoral head force, the great trochanteric force and the vastus lateralis force [19, 29].

2. *Sideways falling* for this test, an existing standardized protocol was used [19]. The aim is to simulate the effect of one of the most common injuries occurring to patients (e.g., falling out of bed). For this task, the shaft is oriented at 10° respect to the horizontal plane (representing the ground) and the femoral neck is internally rotated by 15°. The greater trochanter is then constrained along the vertical axis to represent the contact with the ground, and the bone is left free to rotate in terms of abduction–adduction and to translate on the horizontal plane. In the distal part, the femur is fixed against internal–external rotation around its shaft axis but it is free to slide. To apply the load, a surface of 200 mm^2 is defined on the inferior surface of the femoral head and 5000 N are applied there [30–33].

3. *Four-point bending* this test simulates the boundary conditions of the standard experimental test used to evaluate bone resistance, in particular bending stiffness and strength of slender structures (such as long bones). This load condition results in a constant bending moment in the central part of the shaft, and it is used to investigate fracture resistance due to the fact that it can induce a fracture in the central part of the bone. From a clinical perspective, this configuration effectively replicates the forces that can arise during specific situations such as falling onto a small objects or accidentally bumping into furniture corners. Such scenarios are not uncommon, especially in everyday environments, and can subject the femur to unique stress patterns due to the localized impact.

The model involved four equidistant cylinders 80 mm apart from each other, two on the lateral side of the femur and two on the medial one; the femur was then clamped at the distal and proximal part to avoid rotation (see Fig. 2). The load is applied pushing the two cylinders on the lateral side with constant load of 500 N on both cylinders inner part, thus simulating a latero-medial bending [34, 35].

Table 1 Value of the forces used for the gait cycle and relative application point

Force	Fx (N)	Fy (N)	Fz (N)	Application point
Femoral head hip force	− 518.3	381.2	2569.9	Head of the femur
Great trochanteric force	543.4	− 133.8	677.2	Great trochanter
Vastus lateralis force	− 7.5	− 154.7	776.6	Anterior proximal end of the femur

X is the medio-lateral direction, Y is the antero-posterior direction and Z is the proximo-distal direction. The great trochanteric force considers the sum of the abductor farce (Gluteus medius, Gluteus minimus and Gluteus maximus), and the tensor fasciae latae force
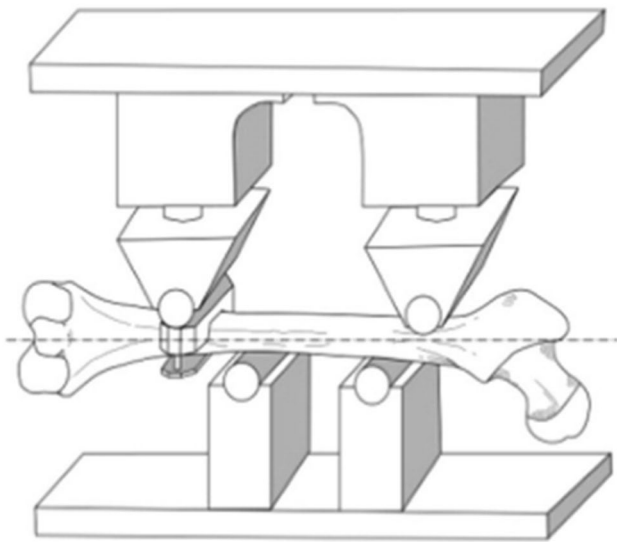
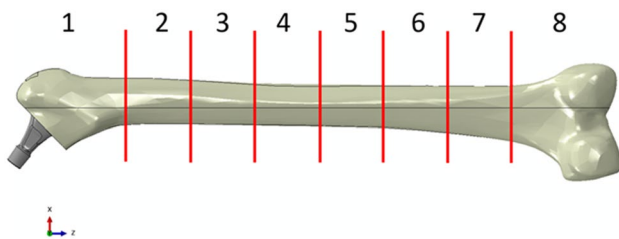**Fig. 2** Graphical representation of the four-point bending test on a femur

Fig. 3 Repartition of the femur in the different regions of interest analyzed

Output and risk of fracture calculation

Average Von Mises stress and strain were considered as outputs for the different simulations, in order to evaluate the implications of the different boundary conditions on the incidence of PFF.

To analyze the von Mises stress, the bone was then subdivided into 8 different regions of interest (ROI) ordered from proximal to distal. The diaphysis was thus divided in regions of 50 mm length, while the proximal epiphysis was 90 mm (see Fig. 3). For the gait and falling tasks, all the ROIs were analyzed; for the four-point bending, the stress was analyzed in the region between the internal cylinders in order to avoid the effects due to proximity of the force applications surfaces.

As the fracture of bone has been proven to be strain-determined [36], a scalar risk for fracture (RF) was calculated as the ratio between the maximum principal strain in the femur shaft (either compressive or tensile) and the ultimate strain corresponding to the material involved [37, 38]. The

ultimate strains for bones are different for compressive and tensile conditions: [30, 36], in details is 0.0104 for compression and 0.0073 for tension.

The overall risk for fracture of the proximal femoral was thus evaluated as the maximum value between the tension and compression RF.

Finite-element analysis

Each model was meshed using linear tetragonal elements. Abaqus/Standard (Dassault Systèmes, Vélizy-Villacoublay, France) was used to perform all the finite-element simulations.

Results

The results are here reported for each task.

Gait cycle

Considering physiological bone, the anatomical stem (Type 6) and the short anatomical stem with femoral neck preservation demonstrated performances comparable with the native model in terms of stress distribution (see Figs. 4 and 5); the average von Mises stress distribution in region 3 is indeed comparable with native configuration for these stems. On the opposite, the double-wedge stem (Type 2) demonstrated a reduction of average von Mises stress in the proximal femoral area (Zones 1–5): these results, therefore, are representative of the phenomenon of stress shielding, often observed during the follow-up of this kind of straight stems [39]. It is furthermore possible to observe, comparing Type 2 stem design with the others, an overall non-homogeneous stress distribution with stress concentrations found in a smaller femoral area.

Rf (see Fig. 6) is almost independent by the implant design (it is almost constant for the native, and only changes slightly for the osteoporotic). Addressing then the osteoporotic bone, a 5% increase of the average von Mises stress can be noted in native, Type 6 and short anatomical stem with femoral neck preservation models; Type 2 stem, instead, returned an increase of the average stress up to 10%.

Sideway falling

Addressing physiological bone quality, the native model returned the highest stress to be concentrated in the femoral neck (see Figs. 7 and 8); this is reasonably in agreement with the boundary conditions involved. The presence of a prosthetic stem, instead, act as an inner support in the femur: it is indeed possible to notice the absence of the area of high stress found in the native model, finding however higher stresses in the

Fig. 4 Graphical representation of Von Mises Stresses relative to "Gait Cycle" task, for the different stem configurations (with healthy bone properties)
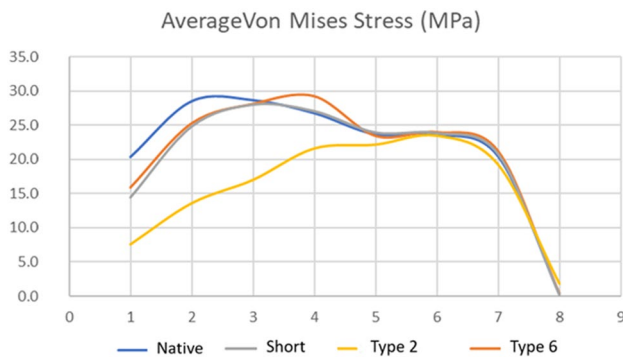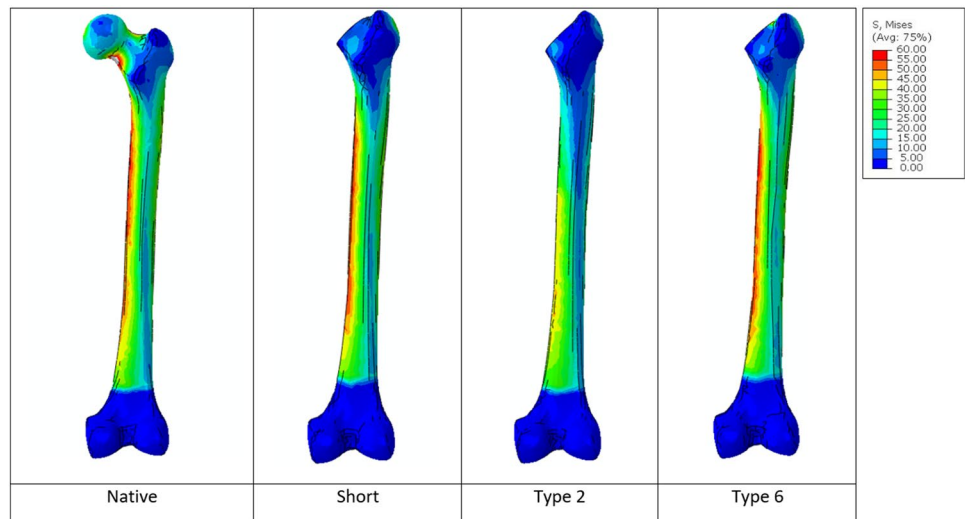

Fig. 5 Average Von Mises Stress of the different ROIs for the "Gait Cycle" task, for the different stem configurations (with healthy bone properties)
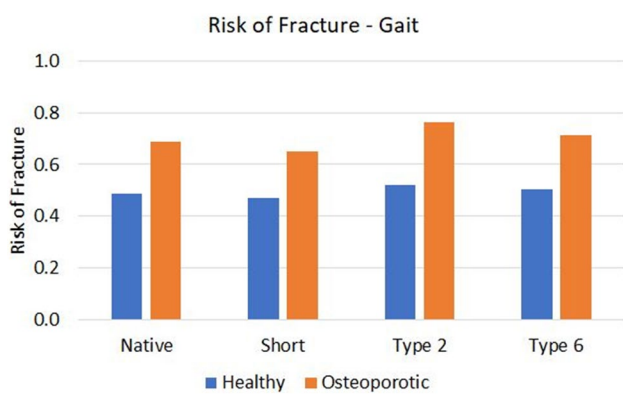

Fig. 6 Risk of Fracture for the "Gait Cycle" task, for the different stem configurations in case of healthy and osteoporotic bone

bone regions corresponding to the stem tip for Type 6 stem (in Zone 2) and for short anatomical stem with femoral neck preservation (in Zone 1). The Type 2 stem, instead, did not return remarkable stress concentrations in the metaphyseal and diaphyseal areas.

Addressing RF (see Fig. 9), in the central bone region the short stem presents the highest values but still relatively low (0.4).

In the osteoporotic bone, an overall increase of the average stress can be noted in all models, mainly focused in the trochanteric region. For Type 6 and short stem, no significant differences in stress distribution can be noted compared to physiological bone; Type 2 stem design instead returned the highest rise of stress in Zone 1 and 3 compared to its physiological counterpart, also reflected in the RF values found (see Fig. 9).

Four-point bending (4-PB)

As often implied in this typology of tests, the central region of the shaft (thus the one comprised between the application of the forces) was the one mainly addressed (see Figs. 10 and 11).

In the models with physiological bone properties, the average von Mises stress distribution returned to be comparable for all the configurations. The Type 6 model returned higher stresses in trochanteric area due to the intrinsic features of the prosthesis (see Fig. 11).

In the osteoporotic bone, no significant differences of average stress can be found compared to the physiological results in any of the studied models (see Fig. 11), which emerges as well from the risk of fracture analysis (see Fig. 12).

Discussion

The current literature shows that the use of cementless stems is characterized by a primary stability (due to the press-fit technique) that then evolves into secondary stability after

Fig. 7 Graphical representation of Von Mises Stresses relative to "Sideway Falling" task, for the different stem configurations (with healthy bone properties)
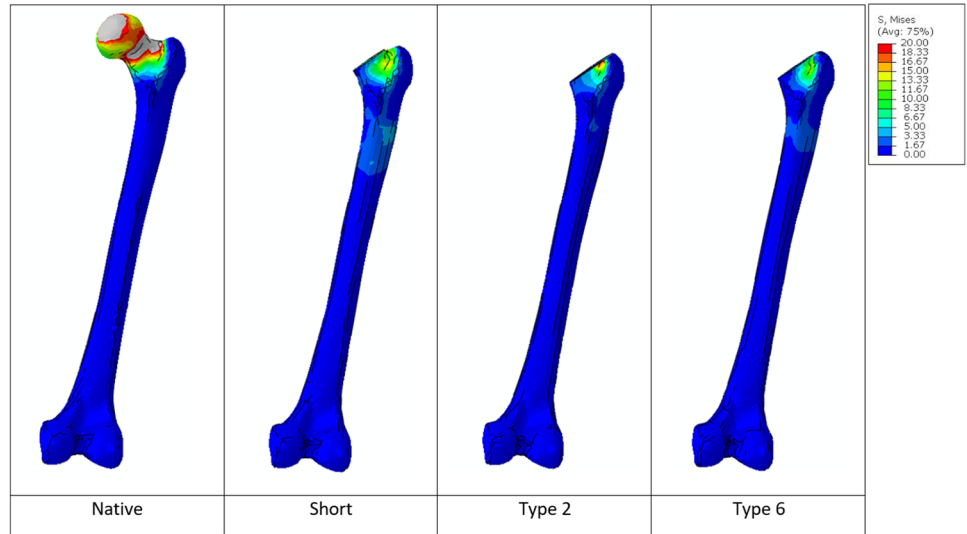

Fig. 8 Average Von Mises Stress of the different ROIs for the "Sideway Falling" task, for the different stem configurations (with healthy bone properties)
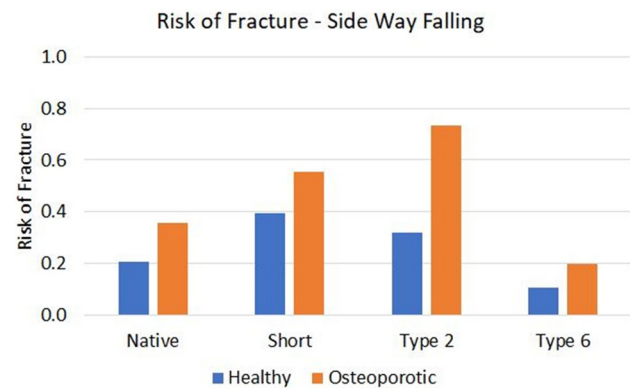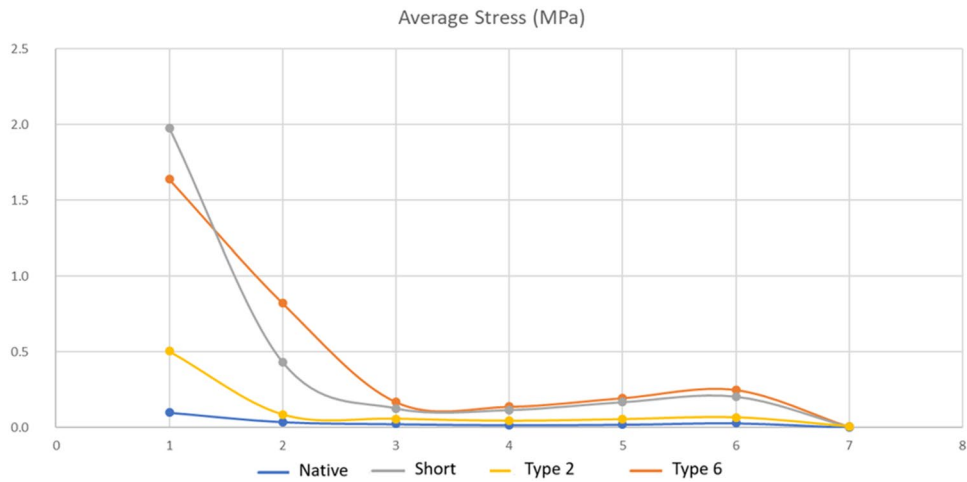

Fig. 9 Risk of Fracture for the "Sideway Falling" task, for the different stem configurations in case of healthy and osteoporotic bone

osteointegration [8, 15]. However, the risk of periprosthetic femoral fracture, which is one of the most frequent complications after a THA implant surgery [1, 14, 15, 19], is reported to be higher for cementless stems during both intra-operative and post-operative periods (within 6 months) if compared to cemented fixation [14, 15, 19].

The data reported in the literature are mainly based on registries or databases. These data present, however, several limitations that could affect their interpretation: in detail, the effect of patients' confounding factors [14, 15], the eventual absence of detailed surgical data (which may be relevant as ream-and-broach technique generally remove greater cancellous bone compared with broach-only systems and this difference could affect PFF risk) [6, 14, 15] and limited information concerning stem design, material and coating [6, 14, 26]. Another limitation is related to the fact that the results of a specific stem with poor performances could have an impact on the global results of its whole design category when statistical analysis is performed [14]: affecting the evaluation of the whole category.

The present numerical study, based on finite-element analysis, allow a standardization of the testing protocol and

Fig. 10 Graphical representation of Von Mises Stresses relative to "Four-Point Bending" task, for the different stem configurations (with healthy bone properties)
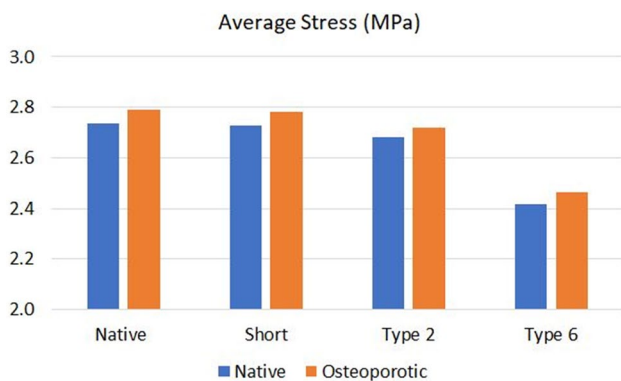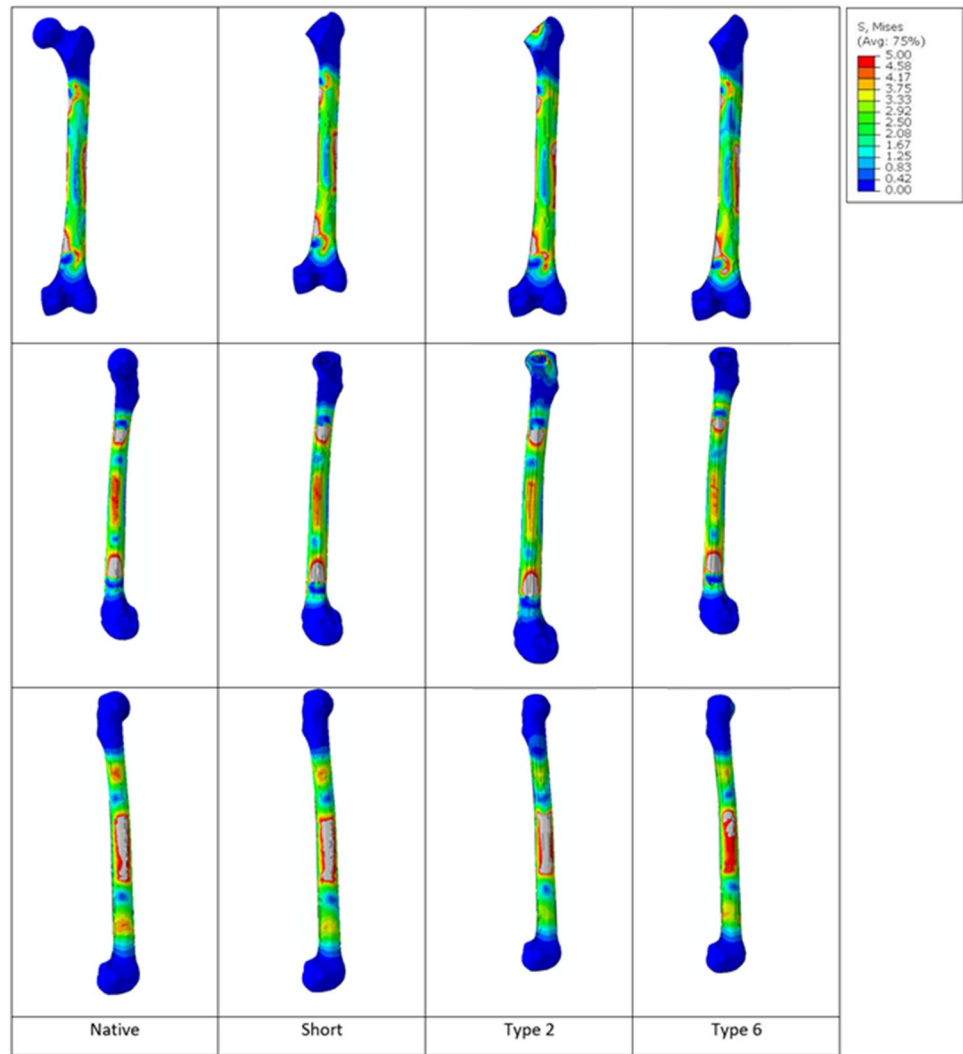

Fig. 11 Average Von Mises Stress of the addressed ROI for the "Four-Point Bending" task, for the different stem configurations in case of healthy and osteoporotic bone
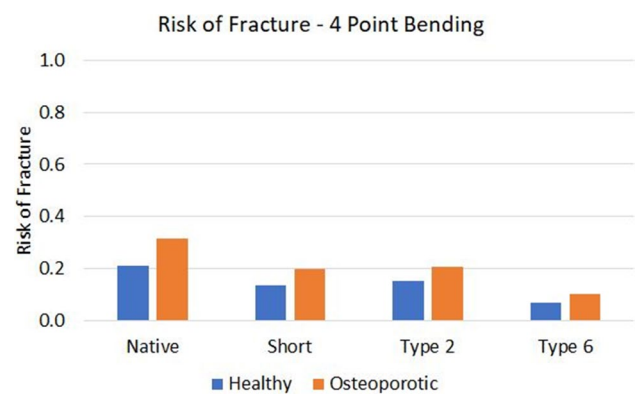

Fig. 12 Risk of Fracture for the "Four-Point Bending" task, for the different stem configurations in case of healthy and osteoporotic bone

boundary conditions, eliminating any confounding elements. The choice to evaluate bone in both physiological and osteoporotic conditions further investigate differences in native

models, as well as analyzing the influence of different stem geometry on PFF in the different situations that may occur during clinical practice.

The results of our study demonstrated that, in physiological bone, during a gait cycle, anatomical and short anatomical stem with femoral neck preservation showed similar performances compared to the native model. On the other hand, double-wedge stem (Type 2) returned a significant reduction of average von Mises stress in the proximal femoral area, already in the initial bone-stem interaction analyzed in this study; this could justify the stress-shielding phenomenon often observed during the clinical follow-up of straight stems, and these results confirm, therefore, the clinical evidence that the anatomic stem design represents a protective factor against stress shielding [6, 8, 39, 40]. These results gave, therefore, further insights on the debate on the reported occurrence of bone resorption in case of anatomical stems (and especially in neck-preserving ones): different authors hypothesized indeed that this phenomenon was not intrinsically related to the implant design, but instead due to errors during surgical planning (in terms of implant size) and surgical technique (related to implant malpositioning) [8, 40]. The positive outcomes obtained in this study for this kind of implants, which were considered as theoretically correctly sized and positioned, prove these hypotheses to be realistic.

Addressing more in detail the Type 2 stems during gait cycle in case of physiological bone, the outcomes demonstrated a non-homogeneous stress distribution, with the tendency to concentrate stresses in a smaller femoral area. In addition, in case of osteoporotic bone, this stem showed an increase up to 10% of the average stress in gait cycle, and the highest difference of stress rise in sideway falling model (with the risk of fracture doubling its value). The clinical implication of these outcomes could, therefore, be interpreted as a theoretical higher risk of PFF: indeed, Carli et al. [14] reported a significant increase of PFF rates in this stem geometry compared to anatomical stem.

When considering the falling configuration in physiological bone conditions, a notable change in the results can be seen. In this traumatic scenario, the use of short or anatomical (Type 6) stems appears to pose indeed a challenge in terms of stress distribution in the neck areas; comparatively, the stress levels for these two types of stems are significantly higher than those observed in the Type 2 or native configurations. Interestingly, it seems that the long straight Type 2 stem is able to effectively prevent excessive loads in this area. On the other hand, when osteoporotic properties are taken into account, this particular stem design carries the highest risk of fracture: this outcome may be due to the concentration of stress around the tip of the stem.

Regarding the four-point bending analysis, no significant differences were observed in the specific central area under investigation: this result implies that the impact caused by this loading condition would not be significantly influenced by the use of different stem configurations, with

only the Type 2 showing slight variations always corresponding to the stem tip.

This study, however, has limitations to be acknowledged. The material properties assigned to the bone were simplified not taking into account variations in bone density, and only one specific bone geometry was considered: this may not encompass the full range of anatomical and material variations that can affect stress and strain distributions.

It is also worth mentioning that this study was conducted exclusively on three specific implant designs. The spectrum of available stems in the market is considerably broader than the models directly examined but, nonetheless, the diverse findings obtained from the simulations offer insights that can be regarded as representative of the broader design classes in terms of their key features. As such, these results still provide valuable and applicable information.

Furthermore, the implementation of static loading conditions in this study does not precisely replicate the exact tasks performed in real-life scenarios. Rather, it aims to simulate a worst-case scenario of the loads involved in such activities. This static nature of the loading conditions could potentially overlook the dynamic aspects and variations in joint forces experienced during dynamic movements.

Nevertheless, it is important to emphasize that these limitations were made to maintain a comparative study design and align with existing literature [16–18]. By ensuring consistency in material properties, bone geometry, and loading conditions across all models, any simplifications or assumptions are likely to impact the different stem designs in a similar manner. As a result, the comparative value of the study is preserved despite these inherent limitations.

Conclusion

The present study provided innovative and interesting data concerning the influence of different stem designs during several loading conditions in terms of stress and strain distributions, and periprosthetic femur fracture risk on both physiological and osteoporotic bone. In the models involving physiological bone, anatomical stems exhibited stress distribution similar to the one obtained for the native model while, in contrast, the double-wedge stem displayed uneven stress distribution, which could contribute to prolonged stress shielding. Notably, for osteoporotic bone, the double-wedge stem design exhibited a remarkable increase in average stress during both gait and sideways falling, potentially signifying an augmented theoretical risk of periprosthetic femur fractures.

These findings hold, therefore, promising clinical implications, offering surgeons valuable insights for risk assessment based on the chosen model.

Declarations

Conflict of interest All the authors certify that they have no affiliations with or involvement in any organization or entity with any financial interest or non-financial interest in the subject matter or materials discussed in this manuscript.

References

1. Patsiogiannis N, Kanakaris NK, Giannoudis PV (2021) Periprosthetic hip fractures: an update into their management and clinical outcomes. EFORT Open Rev 6:75–92. https://doi.org/10.1302/2058-5241.6.200050
2. Inacio MCS, Graves SE, Pratt NL, Roughead EE, Nemes S (2017) Increase in total joint arthroplasty projected from 2014 to 2046 in Australia: a conservative local model with international implications. Clin Orthop Relat Res 475:2130–2137. https://doi.org/10.1007/s11999-017-5377-7
3. Kurtz S, Ong K, Lau E, Mowat F, Halpern M (2007) Projections of primary and revision hip and knee arthroplasty in the United States from 2005 to 2030. J Bone Jt Surg 89:780–785. https://doi.org/10.2106/JBJS.F.00222
4. Nemes S, Gordon M, Rogmark C, Rolfson O (2014) Projections of total hip replacement in Sweden from 2013 to 2030. Acta Orthop 85:238–243. https://doi.org/10.3109/17453674.2014.913224
5. Blankstein M, Haimes MA, Nelms NJ (2022) Selecting a press-fit stem for total hip arthroplasty: the rationale and evolution of the modern femoral prosthesis. J Am Acad Orthop Surg 30:e1279–e1290. https://doi.org/10.5435/JAAOS-D-22-00074
6. Knutsen AR, Lau N, Longjohn DB, Ebramzadeh E, Sangiorgio SN (2017) Periprosthetic femoral bone loss in total hip arthroplasty: systematic analysis of the effect of stem design. HIP Int 27:26–34. https://doi.org/10.5301/hipint.5000413
7. Blankstein M, Lentine B, Nelms NJ (2020) The use of cement in hip arthroplasty: a contemporary perspective. J Am Acad Orthop Surg 28:e586–e594. https://doi.org/10.5435/JAAOS-D-19-00604
8. Formica M, Mosconi L, Cavagnaro L, Chiarlone F, Quarto E, Lontaro-Baracchini M, Zanirato A (2022) A 24-year single-centre experience with collum femoris preserving stem: clinical and radiological results in young and elderly population. HIP Int. https://doi.org/10.1177/11207000221093248
9. Ateschrang A, Weise K, Weller S, Stöckle U, de Zwart P, Ochs BG (2014) Long-term results using the straight tapered femoral cementless hip stem in total hip arthroplasty: a minimum of twenty-year follow-up. J Arthroplasty 29:1559–1565. https://doi.org/10.1016/j.arth.2014.02.015
10. Clauss M, Luem M, Ochsner PE, Ilchmann T (2009) Fixation and loosening of the cemented Müller straight stem. J Bone Joint Surg Br 91-B:1158–1163. https://doi.org/10.1302/0301-620X.91B9.22023
11. Pivec R, Issa K, Kapadia BH, Cherian JJ, Maheshwari AJ, Bonutti PM, Mont MA (2015) Incidence and future projections of periprosthetic femoral fracture following primary total hip arthroplasty: an analysis of international registry data. J Long Term Eff Med Implants 25:269–275. https://doi.org/10.1615/JLongTermEffMedImplants.2015012625
12. Abdel MP, Watts CD, Houdek MT, Lewallen DG, Berry DJ (2016) Epidemiology of periprosthetic fracture of the femur in 32 644 primary total hip arthroplasties. Bone Joint J 98-B:461–467. https://doi.org/10.1302/0301-620X.98B4.37201
13. Tanzer M, Graves SE, Peng A, Shimmin AJ (2018) Is Cemented or cementless femoral stem fixation more durable in patients older than 75 years of age? A comparison of the best-performing stems. Clin Orthop Relat Res 476:1428–1437. https://doi.org/10.1097/01.blo.0000533621.57561.a4
14. Carli AV, Negus JJ, Haddad FS (2017) Periprosthetic femoral fractures and trying to avoid them. Bone Joint J 99-B:50–59. https://doi.org/10.1302/0301-620X.99B1.BJJ-2016-0220.R1
15. Thien TM, Chatziagorou G, Garellick G, Furnes O, Havelin LI, Mäkelä K, Overgaard S, Pedersen A, Eskelinen A, Pulkkinen P et al (2014) Periprosthetic femoral fracture within two years after total hip replacement. J Bone Jt Surg 96:e167. https://doi.org/10.2106/JBJS.M.00643
16. Heller MO (2022) Finite element analysis in orthopedic biomechanics. Human orthopaedic biomechanics. Elsevier, Oxford, pp 637–658
17. Innocenti B, Bori E, Armaroli F, Schlager B, Jonas R, Wilke H-J, Galbusera F (2022) The use of computational models in orthopedic biomechanical research. Human orthopaedic biomechanics. Elsevier, Oxford, pp 681–712
18. Bori E, Armaroli F, Innocenti B (2022) Biomechanical analysis of femoral stems in hinged total knee arthroplasty in physiological and osteoporotic bone. Comput Methods Progr Biomed 213:106499. https://doi.org/10.1016/j.cmpb.2021.106499
19. Soenen M, Baracchi M, De Corte R, Labey L, Innocenti B (2013) Stemmed TKA in a femur with a total hip arthroplasty. J Arthroplasty 28:1437–1445. https://doi.org/10.1016/j.arth.2013.01.010
20. Schlegel UJ, Bruckner T, Schneider M, Parsch D, Geiger F, Breusch SJ (2015) Surface or full cementation of the tibial component in total knee arthroplasty: a matched-pair analysis of mid-to long-term results. Arch Orthop Trauma Surg 135:703–708. https://doi.org/10.1007/s00402-015-2190-1
21. Completo A, Simões JA, Fonseca F, Oliveira M (2008) The influence of different tibial stem designs in load sharing and stability at the cement-bone interface in revision TKA. Knee 15:227–232. https://doi.org/10.1016/j.knee.2008.01.008
22. Brihault J, Navacchia A, Pianigiani S, Labey L, De Corte R, Pascale V, Innocenti B (2016) All-polyethylene tibial components generate higher stress and micromotions than metal-backed tibial components in total knee arthroplasty. Knee Surg Sport Traumatol Arthrosc 24:2550–2559. https://doi.org/10.1007/s00167-015-3630-8
23. Innocenti B, Truyens E, Labey L, Wong P, Victor J, Bellemans J (2009) Can medio-lateral baseplate position and load sharing induce asymptomatic local bone resorption of the proximal tibia? A finite element study. J Orthop Surg Res 4:26. https://doi.org/10.1186/1749-799X-4-26
24. Innocenti B, Bori E (2020) Change in knee biomechanics during squat and walking induced by a modification in TKA size. J Orthop 22:463–472. https://doi.org/10.1016/j.jor.2020.10.006
25. Wilkerson J, Fernando ND (2020) Classifications in brief: the Dorr classification of femoral bone. Clin Orthop Relat Res 478(8):1939–1944. https://doi.org/10.1097/CORR.0000000000001295
26. Khanuja HS, Vakil JJ, Goddard MS, Mont MA (2011) Cementless femoral fixation in total hip arthroplasty. J Bone Jt Surg 93:500–509. https://doi.org/10.2106/JBJS.J.00774
27. Kayabasi O, Ekici B (2007) The effects of static, dynamic and fatigue behavior on three-dimensional shape optimization of hip prosthesis by finite element method. Mater Des 28:2269–2277. https://doi.org/10.1016/j.matdes.2006.08.012
28. Yang Z, Cao J, Yu W, Hou S, Wang G, Lang S, Ding P (2021) Effects of microstructure characteristics on the mechanical properties and elastic modulus of a new Ti–6Al–2Nb–2Zr–0.4B Alloy.

Mater Sci Eng A 820:141564. https://doi.org/10.1016/j.msea.2021.141564

29. Heller MO, Bergmann G, Kassi J-P, Claes L, Haas NP, Duda GN (2005) Determination of muscle loading at the hip joint for use in pre-clinical testing. J Biomech 38:1155–1163. https://doi.org/10.1016/j.jbiomech.2004.05.022

30. Ford CM, Keaveny TM, Hayes WC (2009) The effect of impact direction on the structural capacity of the proximal femur during falls. J Bone Miner Res 11:377–383. https://doi.org/10.1002/jbmr.5650110311

31. Courtney AC, Wachtel EF, Myers ER, Hayes WC (1995) Age-related reductions in the strength of the femur tested in a fall-loading configuration. J Bone Jt Surg 77:387–395. https://doi.org/10.2106/00004623-199503000-00008

32. Robinovitch SN, Hayes WC, McMahon TA (1997) Distribution of contact force during impact to the hip. Ann Biomed Eng 25:499–508. https://doi.org/10.1007/BF02684190

33. Bouxsein M, Coan B, Lee S (1999) Prediction of the strength of the elderly proximal femur by bone mineral density and quantitative ultrasound measurements of the heel and tibia. Bone 25:49–54. https://doi.org/10.1016/S8756-3282(99)00093-9

34. Cristofolini L, Viceconti M (2000) Mechanical validation of whole bone composite tibia models. J Biomech 33:279–288. https://doi.org/10.1016/S0021-9290(99)00186-4

35. McNamara BP, Cristofolini L, Toni A, Taylor D (1994) Evaluation of experimental and finite element models of synthetic and cadaveric femora for pre-clinical design-analysis. Clin Mater 17:131–140. https://doi.org/10.1016/0267-6605(94)90136-8

36. Nalla RK, Kinney JH, Ritchie RO (2003) Mechanistic fracture criteria for the failure of human cortical bone. Nat Mater 2:164–168. https://doi.org/10.1038/nmat832

37. Schileo E, Dall'Ara E, Taddei F, Malandrino A, Schotkamp T, Baleani M, Viceconti M (2008) An accurate estimation of bone density improves the accuracy of subject-specific finite element models. J Biomech 41:2483–2491. https://doi.org/10.1016/j.jbiomech.2008.05.017

38. Bayraktar HH, Morgan EF, Niebur GL, Morris GE, Wong EK, Keaveny TM (2004) Comparison of the elastic and yield properties of human femoral trabecular and cortical bone tissue. J Biomech 37:27–35. https://doi.org/10.1016/S0021-9290(03)00257-4

39. Dhillon MS, Jindal K, Kumar P, Rajnish RK, Neradi D (2022) Long-term survival of CLS Spotorno femoral stem: a systematic review of literature. Arch Orthop Trauma Surg 142(6):1239–1251. https://doi.org/10.1007/s00402-021-03975-0

40. Formica M, Cavagnaro L, Basso M, Zanirato A, Palermo A, Felli L (2017) What is the fate of the neck after a collum femoris preserving prosthesis? A nineteen years single center experience. Int Orthop 41:1329–1335. https://doi.org/10.1007/s00264-016-3350-9